



PERGAMON

Available online at www.sciencedirect.com

SCIENCE @ DIRECT®

Solid State Communications 128 (2003) 1–4

solid
state
communications

www.elsevier.com/locate/ssc

Structures of indium oxide nanobelts

Xiang Yang Kong^{a,b}, Zhong Lin Wang^{a,*}

^a*Department of Materials, School of Materials Science and Engineering, Georgia Institute of Technology, 771 Ferst Dr, Atlanta, GA 30332-0245, USA*

^b*School of Materials Sciences and Engineering, Shanghai Jiao Tong University, Huashan Road 1954, Shanghai 200030, People's Republic of China*

Received 3 July 2003; accepted 18 July 2003 by D.E. Van Dyck

Abstract

Indium oxide nanobelts of growth directions of [100] type (majority) and [120] type (minor) have been found. The two types of nanobelts have the top and bottom surfaces being (001), while the [100] type nanobelts have side surfaces of (010) and a rectangular cross-section, and the [120] type nanobelts have a parallelogram cross-section. The nanobelts have a perfect crystal structure without the presence of line or planar defects.

© 2003 Elsevier Ltd. All rights reserved.

PACS: 68.65. – k; 81.07. – b; 07.10.Cm

Keywords: A. Nanobelt; A. In₂O₃

Indium oxide is an important transparent conducting oxide (TCO) material that has applications in optoelectronics [1–3] and flat panel displays due to its high electrical conductivity and high optical transparency [4]. Indium oxide also has very interesting superconductor–insulator transition behavior at low temperature and in low dimension [5]. Electronic structures of In₂O₃ have been investigated by first principle calculations [6,7]. Since the first report of nanobelt structures of In₂O₃ in 2001 [8], there are a few reports related to nanostructures of In₂O₃, but a diversity exists regarding the growth morphology and crystallographic growth directions. Pan et al. [8] reported the ⟨100⟩ growth nanobelts, with the side and top surfaces being {100}. Liang et al. [9] reported the growth of [110] nanofibers, some of which have {100} side surfaces. The nanowires reported by Li et al. [10] have been attributed to grow along [110]. The In₂O₃ nanotubes reported by Li et al. [11] have a growth direction of [111]. The nanowires reported by Dai et al. [12] are also considered to grow along [111]. To correctly define the nanostructures grown by the

solid–vapor phase deposition, in this paper, we have used high-resolution electron microscopy to study the detailed microstructure of In₂O₃ nanobelts to clearly define their structures. Nanobelts of growth directions of [100] type and [120] types have been found. The two types of nanobelts have the top and bottom surfaces being (001), while the [100] type nanobelts have side surfaces of (010), and the [120] type nanobelts have side direction parallel to the top surface being [2 $\bar{1}$ 0]. The nanobelts have a perfect crystal structure without the presence of line or planar defects.

Our samples were synthesized based on thermal evaporation of oxide powders without catalyst. The original source In₂O₃ powders were placed at the center of an alumina tube that was inserted in a horizontal tube furnace, where the temperature, pressure and evaporation time could be controlled. The tube furnace was heated to 1400 °C (the melting point of In₂O₃ is about 1910 °C); the tube chamber pressure was kept 300 Torr with Ar flux at about 50 sccm (standard cubic centimeter per minute). The evaporation time was holding in 45 min. During evaporation, the products were deposited onto an alumina plate placed at the downstream end of the alumina tube. The as-deposited products were characterized and analyzed by scanning electron microscopy (SEM) (LEO 1530 FEG), transmission

* Corresponding author. Tel.: +1-404-894-8008; fax: +1-404-894-8008/9140.

E-mail address: zhong.wang@mse.gatech.edu (Z.L. Wang).

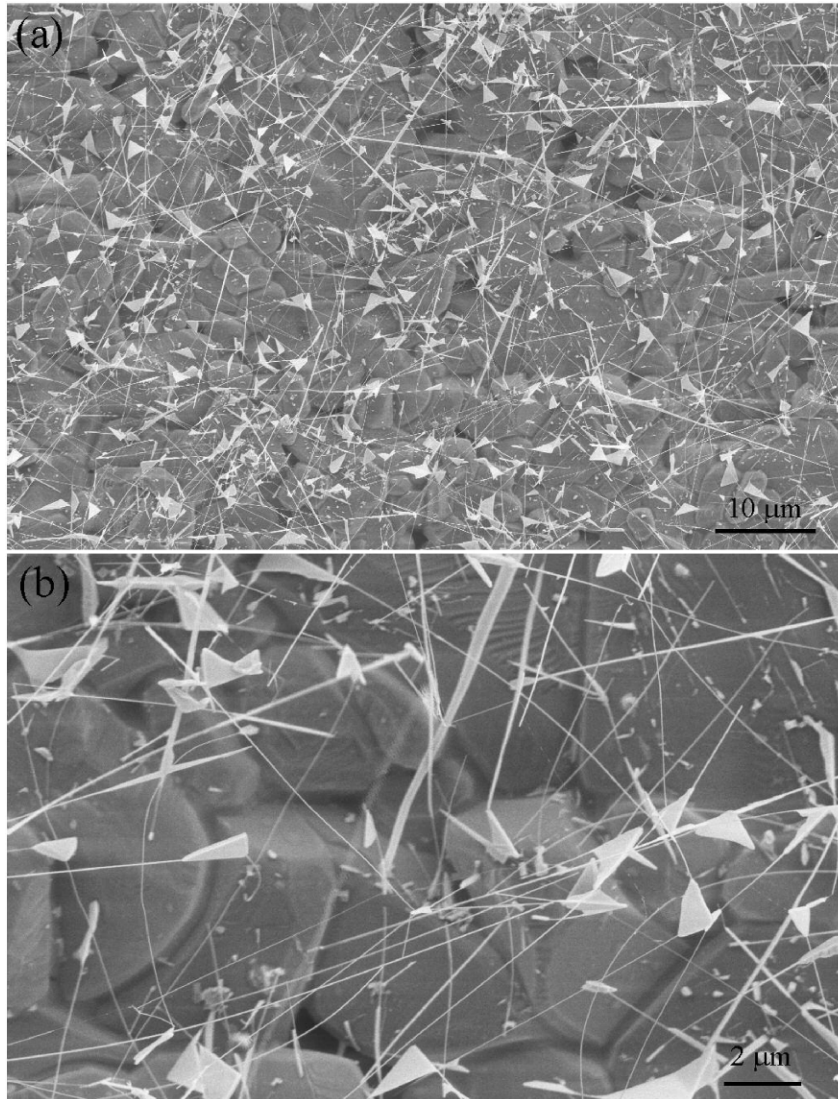


Fig. 1. SEM images of In₂O₃ nanobelts, showing the uniform morphology and growth configuration.

electron microscopy (TEM) (Hitachi HF-2000 FEG at 200 kV and JEOL 4000EX high-resolution TEM (HRTEM) at 400 kV), and energy dispersive X-ray spectroscopy (EDS).

Fig. 1 shows SEM images of In₂O₃ nanobelts deposited on an alumina substrate. The nanobelts are dispersively distributed onto the substrate surface (Fig. 1a), and there appears no correlation among the nanobelts and the substrate. A higher magnification SEM image indicates that the nanobelts have a fairly uniform size distribution, with sizes of 20–40 nm in width and several microns in length. All of the nanobelts are straight and structurally uniform. It is also noticed that there is a triangular sheet in the growth product, from the two corners of which two nanobelts are grown along two perpendicular directions.

This type of structure is frequently observed. Such a structure is clearly displayed by TEM image given in Fig. 2a. Electron diffraction from the structure unambiguously indicates their single crystalline structure, and the two nanobelts grow along [100] and [010], their top and bottom surfaces are (001), and the side surfaces are (010) and (100), respectively. The nanobelt has no line or planar defects, while the contrast observed in the low-magnification image is due to strain induced by bending. High-resolution TEM image (Fig. 2b) clearly shows the perfect crystal structure of the nanobelts, without line or planar defects. The high-resolution TEM image also shows that there is no thickness variation across the nanobelt. The profile image shown here also presents a clean and atomically sharp and smooth {100} surfaces. Therefore, the [100] type nanobelts have a

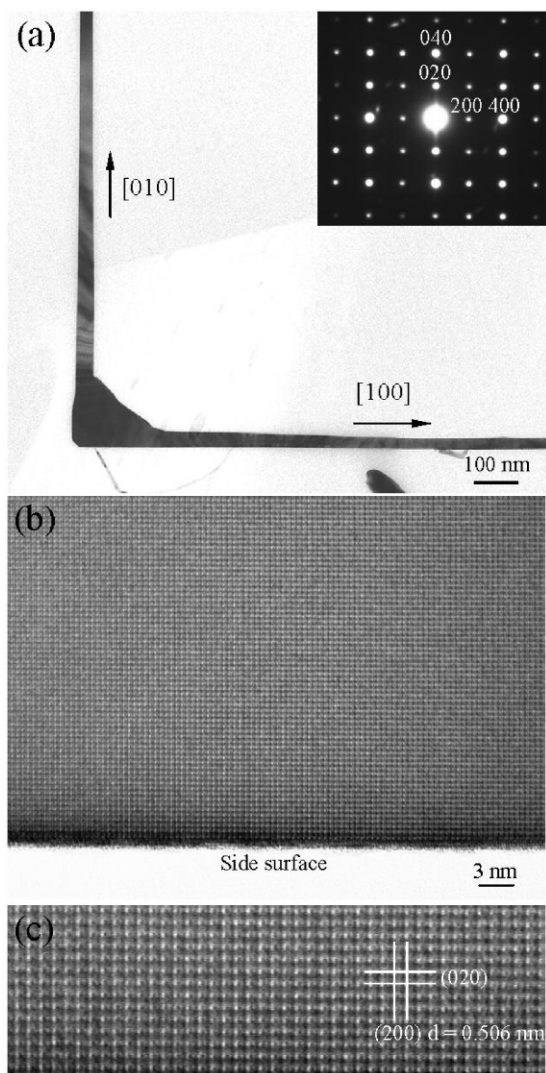


Fig. 2. (a) Low-magnification TEM image and the corresponding electron diffraction pattern from a 'L' shape nanobelt, oriented along [001]. (b) High-resolution TEM image recorded near the side surface of the nanobelt with electron beam parallel to [001]. The flatness of the side surface can be clearly visualized from this profile image. (c) A larger magnification of the TEM image, showing the uniform contrast across the nanobelt.

rectangular cross-section. The [100] type nanobelts are the dominant component of the growth product.

The other type of nanobelts found in the growth product is the [120] type. Fig. 3a shows a low-magnification TEM image of the nanobelt, and the corresponding high-resolution TEM image is given in Fig. 3b, which displays dislocation-free volume. A Fourier transform of the image is given in Fig. 3c, which is indexed to be [001]. The most interesting point is that the nanobelt grows along [120], and its top and bottom surfaces are (001). The image contrast further into the nanobelt is uniform, indicating a uniform

thickness of the nanobelt. The variation in contrast within a distance of ~ 5 nm from the edge of the nanobelt, however, indicates a variation in the projected thickness along [001], which suggests that the side facets of the nanobelt are not parallel to the electron beam direction of [001], and thus the (2 $\bar{1}$ 0) plane may not be the side surface. We can confidently conclude that the side direction of the nanobelt parallel to the (001) top surface is $[2\bar{1}0]$. It is thus suggested that the [120] type nanobelts have a parallelogram cross-section.

Structurally, In_2O_3 has the bixbyite structure (C-rare earth crystal structure) as given in Fig. 4a, the space group symmetry being $Ia\bar{3}$ (206) and lattice constant being 1.0117 nm. Every unit cell contains eight formula units of In_2O_3 : indium atoms occupy Wyckoff positions 8b and 24d, oxygen atoms occupy Wyckoff positions 48e. We have found two types of nanobelts. The projection of the [100] type nanobelt from [001] is given in Fig. 4b. Crystallographically, the (100), (010) and (001) are identical planes with the same surface energy. Due to the unequilibrium growth conditions, the anisotropic growth of the nanobelts along one of the three identical axes is attributed to the growth kinetics. The (100) surface is terminated with either In or oxygen, thus, surface adsorption is expected to balance the In terminated surface. Our TEM image shown in 2b clearly indicates the atomic smoothness of the surface.

The [120] type nanobelt has the same (001) top surface, and its structure model is given in Fig. 4c. There are cations and anions on the side surface, which are distributed in a zig-zag configuration along the surface, thus, the surface is not likely to be atomically flat. This can be seen through the profile TEM image given in Fig. 3b, where the zig-zag atomic structures are visible toward the edge.

One of the important experience encountered in our analysis is the correct observation of the nanobelts. If the nanobelts lay down onto a flat carbon film without a significant degree of tilting, the determined orientation could be the true growth direction. On the other hand, the nanobelt could lay onto the substrate at a small angle that is closely to a zone axis, the electron diffraction determined growth direction would not be the true growth direction but the projected direction perpendicular to the beam. A practical operation to avoid this mistake is to examine a lot of more nanobelts using TEM before a structural configuration is given. This is the reason that we believe that there are diversity in the reported growth directions in the literature.

In conclusion, the microstructures of In_2O_3 nanobelts have been investigated by high-resolution electron microscopy. Nanobelts of growth directions of [100] type (majority) and [120] type (minor) have been found. The two types of nanobelts have the top and bottom surfaces being (001), while the [100] type nanobelts have side surfaces of (010) (rectangular cross-section), and the [120] type nanobelts have a side direction parallel to the top surface being $[2\bar{1}0]$ and an inclined side surface (parallelogram cross-section). The nanobelts have a perfect crystal structure

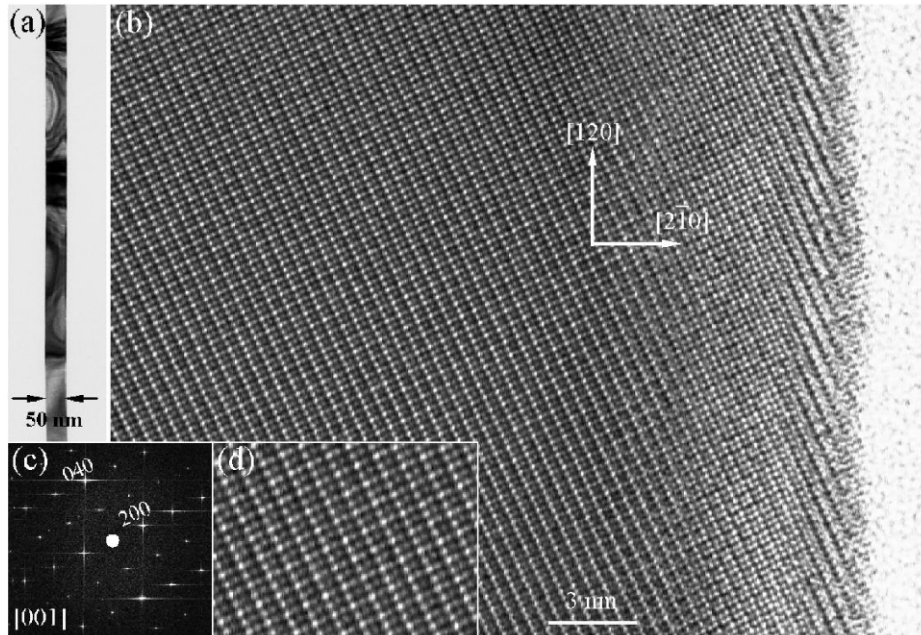


Fig. 3. (a) Low-magnification TEM image of a [120] type In_2O_3 nanobelt. (b) High-resolution TEM image recorded with the incident electron beam parallel to [001]. (c) A Fourier transform of the image given in (b). (d) An enlarged TEM image showing the [001] projected structure of the nanobelt.

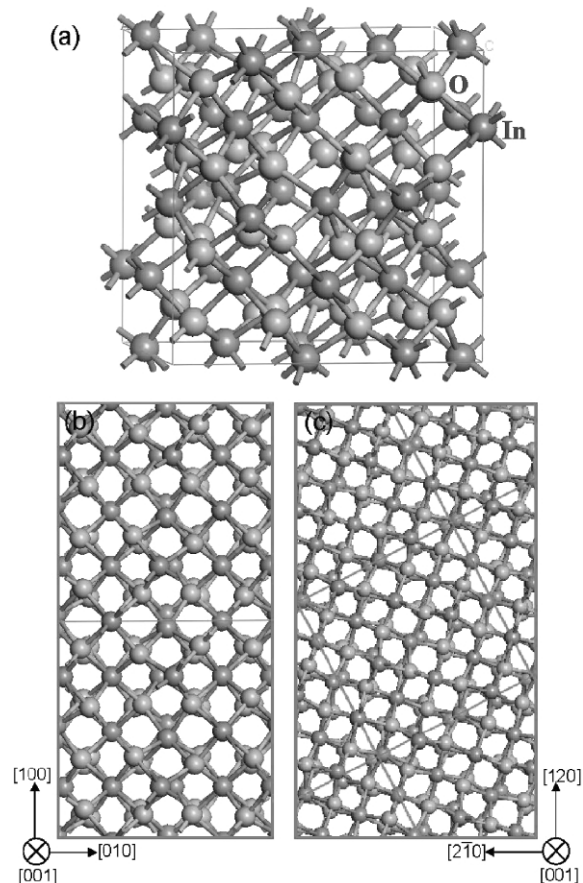


Fig. 4. (a) Unit cell of In_2O_3 . (b) [001] Projected model of the [100] type nanobelts. (c) [001] Projected model of the [120] type nanobelts.

without the presence of line or planar defects. The surfaces of the nanobelts are smooth and without much contamination. Using these structurally controlled nanobelts, a large variety of interesting physical properties can be studied.

Acknowledgements

Research sponsored by NSF NIRT.

References

- [1] S. Ishibashi, Y. Higuchi, Y. Oa, K. Nakamura, *J. Vac. Sci. Technol. A* 8 (1990) 1399.
- [2] K.L. Chopara, S. Major, D.K. Pandya, *Thin Solid Films* 102 (1983) 1.
- [3] J.L. Yao, S. Hao, J.S. Wilkinson, *Thin Solid Films* 189 (1990) 227.
- [4] Z.M. Jarzebski, *Phys. Status Solidi A* 71 (1982) 13.
- [5] V.F. Grantmakher, M.V. Golubkov, V.T. Dolgoplov, G.E. Tsydynzhapov, A.A. Shashkin, *JETP Lett.* 68 (1998) 363.
- [6] H. Odaka, S. Iwata, N. Taga, S. Ohnishi, Y. Kaneta, Y. Shigesato, *Jpn. J. Appl. Phys., Part 1* 36 (1997) 5551.
- [7] I. Tanaka, M. Mizuno, H. Adachi, *Phys. Rev. B* 56 (1997) 3536.
- [8] Z.W. Pan, Z.R. Dai, Z.L. Wang, *Science* 291 (2001) 1947.
- [9] C. Liang, G. Meng, Y. Lei, F. Phillipp, L. Zhang, *Adv. Mater.* 13 (2001) 1330.
- [10] C. Li, D. Zhang, S. Han, X. Liu, T. Tang, C. Zhou, *Adv. Mater.* 15 (2003) 143.
- [11] Y. Li, Y. Bando, D. Golberg, *Adv. Mater.* 15 (2003) 581.
- [12] L. Dai, X.L. Chen, J.K. Jian, M. He, T. Zhou, B.Q. Hu, *Appl. Phys. A* 75 (2002) 687.